PERGAMON

Solid-State Electronics 46 (2002) 61–68

SOLID-STATE ELECTRONICS

Carrier transport and luminescence in composite organic–inorganic light-emitting devices

Alexander Shik, San Yu, Erik Johnson *, Harry Ruda, Edward H. Sargent

Electrical and Computer Engineering, University of Toronto, 10 King's College Road, Toronto, Ont., Canada M5S 3G4

Received 25 February 2000; received in revised form 18 July 2001

Abstract

A model is presented to explain the light-current–voltage characteristics of composite light-emitting structures. These structures are composed of a conducting polymer matrix impregnated with a sheet of inorganic quantum dot nanocrystals. Such structures were reported to exhibit emission characteristics which were extremely promising but, at the same time, not explicable using available models. We present a generalized model that can describe the salient observed characteristics.

Keywords: Polymer; Nanocrystal; Quantum dot; Light emission

1. Introduction

Light-emitting polymers have been the subject of considerable interest over the past decade (see, e.g., Ref. [1]). Because of their light weight and excellent mechanical properties, they are ideal candidates for applications which require portability. The ease of processability and flexibility in thin film form of polymers (e.g. spin-on or ink-jet printed deposition [2]) contrasts starkly with the stringent requirements of vacuum epitaxial growth of monocrystalline semiconductor heterostructures. Flexible substrates lend themselves to innovative designs for end products and processing based on continuous coating of large-area surfaces. This physical flexibility is matched by functional versatility: a wide variety of compounds can be fashioned using synthetic methods, with energy gap and ionization potential being tuned by chemical modification of polymer chains.

Unfortunately, due to the low carrier mobility and low probability of radiative decay of excitons, the external quantum yield of luminescence in polymer structures is small. This limits immediate and wide-ranging development of the devices. To overcome this drawback, a new degree of freedom has been introduced to the realm of conducting light-emitting polymers: the incorporation of an inorganic component in order to form composite structures [3]. This approach takes advantage of the inherent benefits of each constituent: the polymer processing advantages, including solution processing, large-area compatibility, and physical and functional versatility are preserved, and are augmented by the charge transport, interface control, quantization effects, and high radiative efficiency of inorganic compounds. Inorganic nanocrystals such as CdS [4], CdSe [3,4] or CdS/CdSe [5] or ZnS/CdSe [6] core-shell structures consisting of a few monolayers of CdS (or ZnS) surrounding a CdSe core are particularly interesting model systems and represent a promising base technology.

In recent years, the luminescent properties of the above-mentioned composite system have been investigated experimentally in a number of research groups. Several interesting properties have been reported:

- simple relationships were found between nanocrystal size and emission spectrum [5,6,8];
- the relative intensity of luminescence from the nanocrystals and polymer matrix depends strongly on the

* Corresponding author. Tel.: +1-416-946-7017; fax: +1-416-971-3020.

E-mail address: erik.johnson@utoronto.ca (E. Johnson).

0038-1101/02/$ - see front matter
PII: S0038-1101(01)00289-1

applied voltage, increasing with increased forward bias [5,7];
- the electroluminescence spectrum may either coincide with that of the photoluminescence [7,8] or have a noticeable red shift [5];
- slow turn-on (minutes) and memory effects [5] are observed.

These characteristics, with the exception of the first one, have not yet had the benefit of a systematic theoretical interpretation.

In the present work we analyze luminescence-related phenomena in composite systems. Our model can explain observed effects and suggests ways to increase the effectiveness of polymer-based light-emitting devices.

2. Physical model of a composite structure

We consider theoretically the luminescence of spherical nanocrystals embedded in a semiconducting polymer. We invoke the analogy between polymers and crystalline semiconductors [1], associating the highest occupied and lowest unoccupied molecular orbitals with the valence and conduction bands, respectively. In this approach, our system has much in common with heterojunction quantum dots whose luminescence properties have been already discussed, particularly in connection with the physics of quantum dot lasers [9].

There are, however, important distinctions between the nanocrystal-in-polymer system and the purely inorganic quantum dot system which do not allow direct application of existing theory to the hybrid system considered herein. The excitation of non-equilibrium carriers in quantum dots (nanocrystals) involves two stages: transport to nanocrystals, followed by capture into the potential well of nanocrystal. In most semiconductors the first stage is fast and capture phenomena play the limiting role. This system is described in terms of quasi-levels of delocalized electrons and holes used in standard electron device theory.

The low mobility of carriers in conducting polymers changes the physical picture of non-equilibrium carrier transport to the nanocrystals. In this case, the provision of carriers to the nanocrystals will be limited by transport rather than capture. The spatial distribution of carrier concentration is no longer described using quasi-equilibrium models; instead, it should be found from the continuity equations as it is done in Lampert's theory of current injection [10] or of p–n-junctions with a very high concentration of recombination centers [11].

In this work, we apply these methods in order to find the distribution of non-equilibrium carriers and the quantum yield of electroluminescence in a composite structure containing semiconductor nanocrystals in a polymer matrix. We consider the structure shown schematically in Fig. 1. Here the polymer matrix with dielectric constant ε occupies the layer $0 < x < L$ confined by two planar electrodes across which is applied voltage V. The electrode at $x = 0$ injects electrons; the electrode at $x = L$ injects holes. To give a formal description of this fact, we assume that the contacts always maintain constant concentration of corresponding carriers at their surfaces:

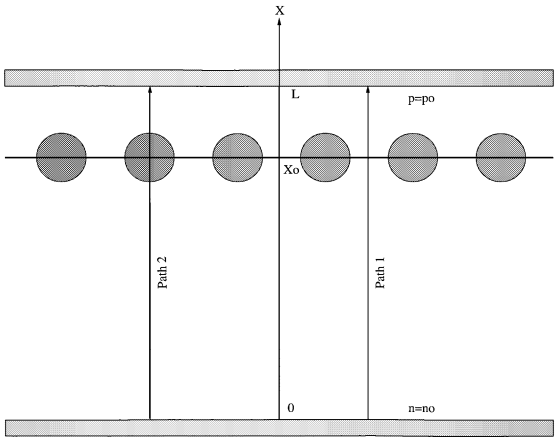

Fig. 1. Schematic of a polymer film with embedded nanocrystals. Broken lines 1 and 2 show trajectories crossing and avoiding nanocrystals (see in the text).

$$n(x = 0) = n_0; \qquad p(x = L) = p_0. \tag{1}$$

Spherical nanocrystals of radius a are embedded in the matrix. In reported experiments, nanocrystals are often distributed not throughout the entire volume of a polymer film, but occupy a layer near one electrode, typically the cathode [5,8]. We suppose therefore that the nanocrytals lie in one plane $x = x_1$. We let d be the average linear spacing between nanocrystals and $N \sim d^{-2}$—their density per unit area.

3. Qualitative picture

We first consider the qualitative picture of non-equilibrium phenomena in the system of Fig. 1. In the first moment after applying the voltage V, the electric field between electrodes is uniform. From Eq. (1), the electron and hole fluxes from the electrodes are, respectively, $n_0\mu_n V/L$ and $p_0\mu_p V/L$ where $\mu_{n,p}$ are the carrier mobilities. If neutral nanocrystals are characterized by the capture cross-sections $\sigma^0_{n,p}$, then the capture rates for electrons and holes in the first moment are $n_0\mu_n\sigma^0_n V/L$ and $p_0\mu_p\sigma^0_p V/L$ and are generally different. If the rate for electrons is higher, the nanocrystals acquire some negative charge Q. This changes the potential distribution in the system. Additional electric field arises which attracts holes to nanocrystal and inhibits the

capture of electrons. Q will reach a stationary value such that fluxes of electrons and holes into each nanocrystal are equal. The charge of non-equilibrium carriers in the polymer matrix is also the source of the perturbation of the electric field from constancy.

Thus, stationary non-equilibrium phenomena in our system occur in a complicated electrostatic potential $\varphi(\mathbf{r})$ which consists of three components: the uniform electric field of electrodes Vx/L, the space charge field created by non-equilibrium carriers, and the Coulomb potentials of nanocrystals. Let E be the external electric field at the nanocrystals determined as a sum of first two components. Depending on the parameters E and Q, three different situations shown in Fig. 2 can arise:

1. Small Q, when E exceeds the electric field of a nanocrystal at its interface $E_+ \sim Q/(\varepsilon a^2)$ (Fig. 2a).
2. Intermediate Q, when E is less than E_+ but exceeds the maximal electric field of nanocrystals at the line (path 1 in Fig. 1) running from one electrode to the other at a maximal distance from nanocrystals $E_- \sim Q/(\varepsilon d^2)$ (Fig. 2b).
3. Large Q, when E is less than E_- (Fig. 2c).

In the first case the potential varies monotonically along all paths between electrodes. Both electrons and holes can move through the entire sample and need not overcome a potential barrier to reach the nanocrystals. In the second case, the potential is monotonic along path 1 between nanocrystals but non-monotonic along path 2 crossing a nanocrystal. In this case, those carriers which move along paths which do not cross nanocrystals have no barriers on their way. To be captured by a nanocrystal and recombine, electrons must overcome a potential barrier Δ_r. As a result, the current–voltage characteristic is activationless but the recombination rate contains a small activation factor $\exp(-\Delta_r/kT)$. Finally, for large Q both the current and the recombination rate contain activation factors with the corresponding energies Δ_d and Δ_r ($\Delta_d < \Delta_r$). Identifying Δ_d and Δ_r with the drift and recombination barriers widely used in the theory of inhomogeneous semiconductors [12], we can say that for small Q neither drift nor recombination barriers are present, for intermediate Q only recombination barriers occur, and for large Q both types of barriers exist in the system.

There exists a direct relationship between the character of the band diagram and the quantum yield of luminescence from nanocrystals. For low mobility and, hence, short mean free path of the carriers, electron (hole) trajectories are exactly antiparallel (parallel) to the electric field lines. This means that in the steady state each nanocrystal is characterized by both incoming and outgoing lines and whose ratio is given by $\mu_n\sigma_n^0/\mu_p\sigma_p^0$. This occurs only for $E > E_+$ since the presence of a recombination barrier implies an absence of incoming lines. For a large difference between $\mu_n\sigma_n^0$ and $\mu_p\sigma_p^0$, E will be close to E_+ or $Q \sim \varepsilon E a^2$.

The electric field lines connecting two electrodes in between nanocrystals correspond to electrons or holes

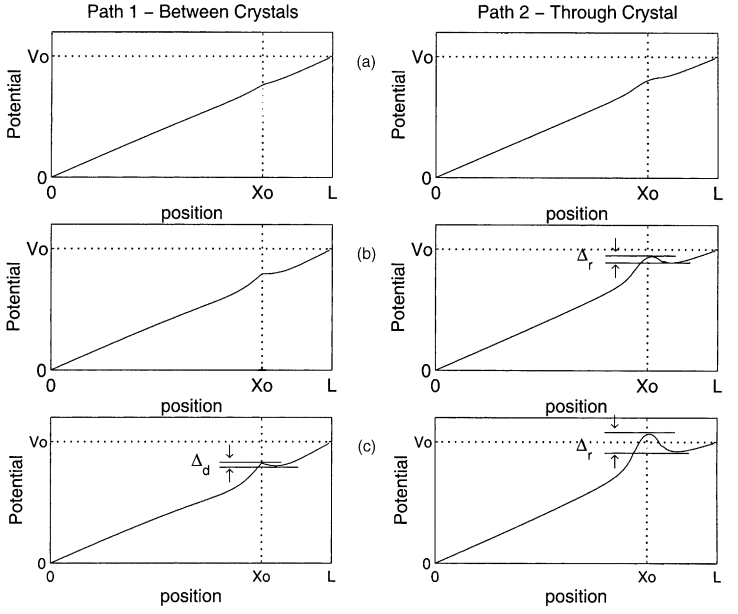

Fig. 2. The potential profile between electrodes along line 1 (left figures) and line 2 (right figures): (a) small Q ($V/L > E_+$); (b) intermediate Q ($E_- < V/L < E_+$) and (c) large Q ($V/L < E_-$).

escaping recombination in nanocrystals. The external quantum yield of recombination in nanocrystals η_1 is then less than unity even if the ratio of the radiative to the total recombination rate inside each nanocrystal is unity, i.e. $\beta_1 = 1$. In our model, in which nanocrystals lie in a single plane, this will be always the case until $\Delta_d = 0$. All carriers injected into the sample will recombine in the nanocrystals only if simultaneously $\Delta_r = 0$ and $\Delta_d > 0$, which is not possible. A single plane of nanocrystals with the "coverage factor" of nanocrystals $\pi N a^2 < 1$ cannot, therefore, provide complete transformation of current into light, i.e. it is not possible that $\eta_1 = 1$. This can be achieved by multi-layer coverage which will give rise to a more complicated potential profile. This requires a more detailed analysis to be performed elsewhere. Here we consider the important generalizable features of carrier capture and recombination inside our single-layer system.

If the sample temperature is not very high, even the small recombination barrier Δ_r suppresses the electron capture rate enough to compensate a large initial asymmetry in electron and hole capture rate. Thus we may expect that, for a large asymmetry, V/L will be close to E_+, or $Q \sim \varepsilon V a^2/L$.

If the concentration of nanocrystals is low enough that $a \ll d$, then the net charge Q, which influences strongly the capture processes, will leave almost untouched the carrier motion through the $x = x_1$ plane far from the nanocrystals. Since the total surface charge density Q/d^2 is much less than $\varepsilon V/L$, the average electric field in the system also remains unchanged: it is equal to V/L at both sides of the $x = x_1$ plane.

The only noticeable effect of nanocrystal charging is to change the effective cross-sections $\sigma_{n,p}$. Their new stationary values must satisfy the relation:

$$\frac{\sigma_n}{\sigma_p} = \frac{\mu_p p_0}{\mu_n n_0} \tag{2}$$

reflecting the equality of electron and hole recombination fluxes.

It is reasonable to assume that for neutral nanocrystals $\sigma_n^0 \sim \sigma_p^0 \sim a^2$ so that for a low concentration of nanocrystals only small part of electron and hole fluxes recombine in the nanocrystals. For charged nanocrystals the situation may be different. If $\mu_p p_0 \ll \mu_n n_0$, then recharging increases σ_p noticeably (e.g., for point defects the cross-section for attractive centers is typically 2–3 orders of magnitude larger than for neutral ones [13]). In this case even for $a \ll d$ the product $\sigma_p d^{-2}$ may exceed unity. This implies that all holes are captured by nanocrystals and recombine. Since the total electron flux exceeds the hole flux, some electrons do not recombine and reach the anode, giving an additional contribution to the current density j. As a result, $j \simeq e\mu_n n_0 V/L$, the recombination flux, is equal to $\mu_p p_0 V/L$. The quantum yield of luminescence, i.e. the number of photons emitted from nanocrystals per one electron passing through the structure, is given by

$$\eta_1 \simeq \beta_1 \frac{\mu_p p_0}{\mu_n n_0} < \beta_1. \tag{3}$$

For the opposite case $\mu_p p_0 \gg \mu_n n_0$ the numerator and denominator in Eq. (3) should be exchanged. Thus, the maximal intensity of luminescence can be reached in symmetric structures with $\mu_p p_0 \simeq \mu_n n_0$.

4. Quantitative analysis

Now we consider in more detail the non-equilibrium phenomena described in the previous section. We obtain quantitative expressions for the quantum yield of luminescence. The processes taken into account should be extended to include recombination in the polymer matrix, a mechanism which we have so far ignored and will initially consider while neglecting the effect of charged nanoparticles on carrier motion. Because of this simplification, the results of this investigation are applicable most accurately to systems with a low planar density of nanocrystals ($a \ll d$). The matrix recombination rate will be described by the standard bimolecular formula $\gamma n(x) p(x)$. The spatial distributions of non-equilibrium carriers $n(x)$ and $p(x)$ are to be found from the continuity equations

$$\mu_n \frac{\mathrm{d}(nE)}{\mathrm{d}x} = -\gamma np; \tag{4}$$

$$\mu_p \frac{\mathrm{d}(pE)}{\mathrm{d}x} = \gamma np, \tag{5}$$

whereas the spatial distribution of electric field $E(x)$ is given by the Poisson equation

$$\frac{\mathrm{d}E}{\mathrm{d}x} = \frac{4\pi e}{\varepsilon}(n - p). \tag{6}$$

Adding Eqs. (4) and (5), we obtain

$$[\mu_n n(x) + \mu_p p(x)]E(x) = j/e = \mathrm{const}(x), \tag{7}$$

where j is the total current through the structure. The system of equations (4), (6) and (7) must be solved with the boundary conditions (1) and the additional requirement

$$\int_0^L E(x)\,\mathrm{d}x = V. \tag{8}$$

Before drawing particular conclusions regarding carrier capture by and luminescence from nanocrystals, we consider first the distribution of non-equilibrium carriers which would exist in the absence of nanocrys-

tals. Depending on the intensity of matrix recombination, two opposite cases should be considered. If

$$\frac{\gamma(n_0\mu_n + p_0\mu_p)L^2}{\mu_n\mu_p V} \ll 1, \tag{9}$$

then recombination in the polymer matrix affects only a small fraction of injected carriers and can be neglected in the calculations. In this case the electron and hole currents $j_n = en(x)\mu_n E(x)$ and $j_p = ep(x)\mu_p E(x)$ remain coordinate independent and the Poisson equation (6) can be written as

$$\frac{dE}{dx}E = \frac{4\pi}{\varepsilon}\left(\frac{j_n}{\mu_n} - \frac{j_p}{\mu_p}\right) \tag{10}$$

subject to the additional conditions $j_n = en_0\mu_n E(0)$; $j_p = ep_0\mu_p E(L)$; and Eq. (8). These permit determination of the integration constant and the two unknown parameters j_n and j_p. Integration gives the following system

$$v = \frac{2}{3}\frac{\left(\frac{i_p}{s}\right)^3 - i_n^3}{\left(\frac{i_p}{s}\right)^2 - i_n^2}; \qquad i_n - i_p = \frac{4}{9}\left(\frac{i_p^2}{s^2} - i_n^2\right) \tag{11}$$

which describes the dependences of dimensionless electron $i_n = (9\varepsilon/32\pi e^2 n_0^2\mu_n L)j_n$ and hole $i_p = (9\varepsilon/32\pi e^2 n_0^2\mu_p L)j_p$ currents on the dimensionless voltage $v = (9\varepsilon/32\pi e n_0 L^2)V$. Here $s = p_0/n_0$ characterizes the asymmetry of the injecting contacts.

For a symmetric system with $s = 1$, electron and hole concentrations are equal everywhere, there is no space charge, and the current–voltage characteristic is always linear: $i_n = i_p = v$. In the case of a strong asymmetry, the minority current is still almost linear in v, but that of majority carriers contain a quadratic part. For instance, at $s \ll 1$

$$i_n \simeq i_p \simeq \frac{3sv}{2}, \quad \text{for } v \ll s;$$

$$i_n \simeq v^2, \quad i_p \simeq \frac{3sv}{2}, \quad \text{for } s \ll v \ll 1; \tag{12}$$

$$i_n \simeq v, \quad i_p \simeq sv, \quad \text{for } v \gg 1.$$

We illustrate these dependencies in Fig. 3 when $s = 1/10$. The low-voltage results, although shown in the figure, may not be valid as the condition (9) fails.

If matrix recombination is very strong (the condition opposite to Eq. (9)), the current near the cathode (anode) consists purely of electrons (holes) and all recombination occurs within a very thin layer $x \simeq x_2$. The exact value of x_2 and the total current–voltage characteristic can be found using the following procedure. Neglecting j_p for $x < x_2$, we integrate Eq. (10) in this region and obtain

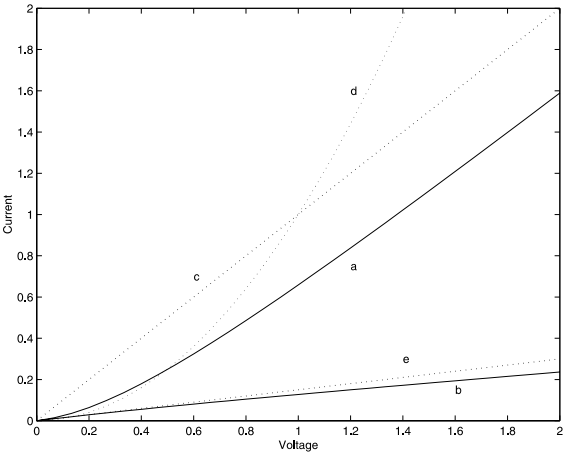

Fig. 3. Current components for the case of weak matrix recombination and $s = 0.1$. Approximate curves from Eq. (13) are shown as dotted lines: (a) i_n; (b) i_p; (c) $i = v$; (d) $i = v^2$ and (e) $i = 3sv/2$.

$$E^2 = 8\pi j_n x/(\varepsilon\mu_n) + j_n^2/(e\mu_n n_0)^2. \tag{13}$$

A similar connection between E and j_p can be obtained for $x > x_2$. Taking into account that for complete recombination $j_n = j_p = j$, and matching the electric field at $x = x_2$, we obtain

$$x_2 = \frac{\mu_n L}{\mu_n + \mu_p} + \frac{\varepsilon j}{8\pi e^2(\mu_n + \mu_p)}\left(\frac{\mu_n}{\mu_p p_0^2} - \frac{\mu_p}{\mu_n n_0^2}\right). \tag{14}$$

To obtain the current–voltage characteristic, we integrate to find $E(x)$ and apply the relation (8). Using the same notation as in Eq. (11), we find

$$v = \sqrt{i}\left\{\frac{1}{\sqrt{1+m}}\left[1 + \frac{4}{9}i\left(1 + m^{-1}s^{-2}\right)\right]^{3/2} - \left(\frac{4}{9}i\right)^{3/2}\left(1 + m^{-2}s^{-3}\right)\right\}, \tag{15}$$

where $m = \mu_p/\mu_n$. For further simplification in a later illustration, we will assume $m \simeq 1$.

For symmetric structures with $s = 1$, Eq. (1) tends to the ideal space charge limited current $i = 2v^2$ at $v \ll 1$ and to Ohm's law $i = v$ at $i \gg 1$. For asymmetric structures, the current–voltage characteristic Eq. (15) at small voltage is also quadratic but does not result in a linear Ohmic dependence for large voltages. However, under these conditions, Eq. (15) itself becomes inadequate. The position of the recombination layer given by Eq. (14) must satisfy the inequality $0 < x_2 < L$. This is always the case for the first term in Eq. (14), which corresponds to the ideal space charge limited current [10] and dominates for a small applied voltage or in symmetric structures with $s = 1$. In asymmetric structures at

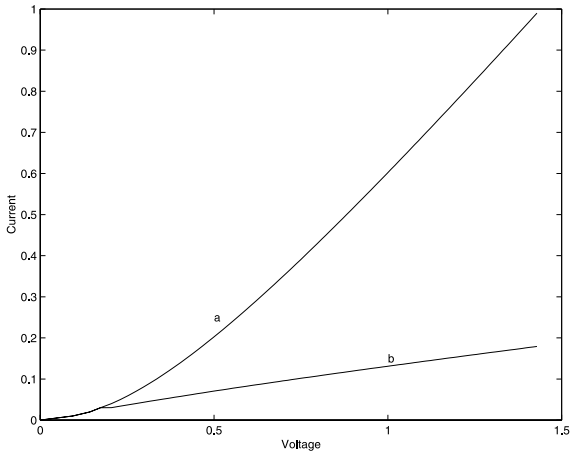

Fig. 4. Current components for the case of strong matrix recombination and $s = 0.1$. Lines: (a) i_n and (b) i_p.

voltages which exceed some critical value v_c, the above-mentioned inequality is violated and Eq. (15) fails.

We consider, as an example, a structure in which electron conductivity dominates, so that $s < 1$. In this case

$$v_c = \frac{3s(1-s^3)}{2(1-s^2)^2}. \tag{16}$$

At larger voltages, x_2 is pinned near L, and the i_n vs v dependence can be found from Eqs. (8) and (13):

$$v = \sqrt{i_n}\left[\left(1+\frac{4}{9}i_n\right)^{3/2} - \left(\frac{4}{9}i_n\right)^{3/2}\right].$$

Since x_2 is pinned near L there is no opportunity to form a hole space charge and the hole current is given by $j_p = e\mu_p p_0 E(L)$ where $E(L)$ is given by Eq. (13) with $j = j_n$. In dimensionless units

$$i_p = s\sqrt{\frac{9}{4}i_n + i_n^2} < i_n. \tag{17}$$

Thus, for a voltage exceeding the critical voltage, there is no longer complete mutual annihilation of electron and hole fluxes. A part of electron current equal to $j_n - j_p$ reaches the anode. The total current in the circuit is then equal to j_n and the recombination current is j_p. The results for $s = 1/10$ are shown in Fig. 4.

5. Quantum yield of luminescence

Using the results of the preceding section, we predict the key quantities of interest in light-emitting structures: the quantum yields of luminescence from nanocrystals η_1 and from the polymer matrix η_2.

The results of Section 4 allow us to find the spatial distributions of non-equilibrium carriers $n(x)$, $p(x)$ and calculate the spatial profile of the recombination rate $\gamma n(x)p(x)$. From this we may obtain the quantum yield of luminescence in the polymer matrix:

$$\eta_2 = \frac{e\beta_2\gamma}{j}\int_0^L n(x)p(x)\,dx = \frac{\beta_2\gamma j_n j_p}{ej\mu_n\mu_p}\int_0^L \frac{dx}{E^2(x)}. \tag{18}$$

Here β_2 is the ratio of the radiative to the total recombination rate in the matrix. In polymers this quantity is determined by the probability of forming excitons in the singlet state and by the efficiency of radiative decay of these singlet excitons [1].

Luminescence from nanocrystals and the parameter η_1 may now be estimated. From Section 4 we can find the electron and hole currents at any point and, in particular, in the plane $x = x_1$ which contains the nanocrystals. As mentioned in Section 3, nanocrystals acquire some charge Q. This changes the effective cross-sections for electrons and holes, equalizing the recombination currents j_r associated with each type of carrier. Though the exact value of j_r cannot be found in a simple phenomenological model, it may be asserted that at any density of nanocrystals it cannot exceed the smaller of the two currents at $x = x_1$: $j_r \leqslant \min\{j_n(x_1); j_p(x_1)\}$. Since the total current j is the sum of electrons and hole components, the efficiency quantum yield of luminescence from the nanocrystals must satisfy the inequality

$$\eta_1 \leqslant \beta_1 \frac{\min\{j_n(x_1); j_p(x_1)\}}{j_n(x_1) + j_p(x_1)}, \tag{19}$$

where the equality is approached for high nanocrystal density.

For weak matrix recombination (Eq. (9)) corresponding to the current–voltage characteristic Eq. (11), the $E(x)$ profile already found in Section 4 permits calculation of η_2 from Eq. (18). In terms of the dimensionless electron and hole currents i_n and i_p the result for identical hole and electron mobilities ($m = 1$) is

$$\eta_2 = \frac{\beta_2\varepsilon\gamma}{8\pi e\mu_n}\frac{i_n i_p}{\left(i_n^2 - i_p^2\right)}\ln\left[\frac{9}{4}\left(\frac{1}{i_n} - \frac{i_p}{i_n^2}\right) + 1\right]. \tag{20}$$

Using the expressions for i_n and i_p from Section 4, it may be shown that η_2 decreases with applied voltage and that at large v, $\eta_2 \sim 1/v$. This occurs because, for $v \to \infty$, the carriers become uniformly distributed over the sample with the concentrations n_0 and p_0, so that j_r approaches the constant value $\gamma n_0 p_0 L$, whereas j increases linearly with the voltage. The right-hand side of Eq. (19) is a constant ~ 1 at low voltages and a constant $\sim \min\{s, 1/s\}$ at high voltages. Thus, the ratio η_2/η_1 decreases with the applied voltage for high voltages. We illustrate the dependence of η_1, η_2 and η_2/η_1 on voltage in Fig. 5 for the particular case of $s = 1/10$. The figure contains no low-voltage region since at small v the condition of weak

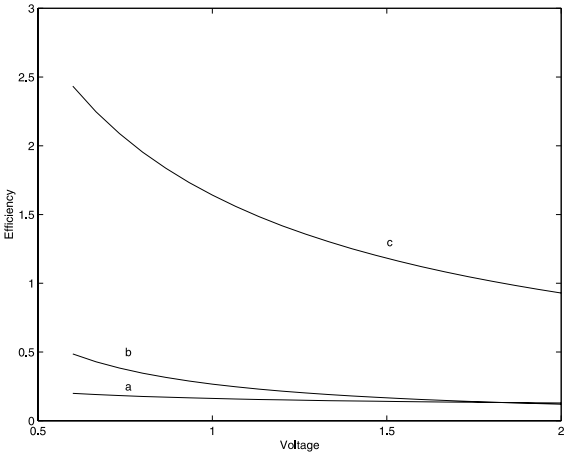

Fig. 5. Quantum yields for the case of weak matrix recombination and $s = 0.1$. (a) η_1/β_1 and (b) η_2/β_2 in units of $\varepsilon\gamma/(8\pi e\mu_n)$; (c) η_2/η_1 in units of $\varepsilon\gamma/(8\pi e\mu_n)$ for $\beta_1 = \beta_2$. Low-voltage results are not shown, as the condition (9) no longer holds as $v \to 0$.

matrix recombination Eq. (9) fails and the formulae for this limiting case become inadequate.

For a strong matrix recombination when the inequality opposite to Eq. (9) is satisfied, η_2 is close to β_2. Recombination in the nanocrystals is strongly suppressed since almost everywhere in the sample either j_n or j_p is close to zero. This is not the case near x_2, so that for η_1 to be appreciable, the position of the nanocrystal layer x_1 must be close to x_2. Since x_2 shifts with the applied voltage towards the contact with weaker injection (see Eq. (14)), the shift of x_1 in the same direction will cause the quantum yield η_1 to increase.

6. Discussion and recommendations

In the previous section we have presented a theoretical description of non-equilibrium transport and radiative recombination in a composite polymer–nanocrystal system. To reveal the main physical features of the phenomena, we have used a simple model which nevertheless allows us to explain qualitatively some experimental trends summarized in Section 1.

In all cases considered in Section 4, the values of efficiency inside the nanocrystals and polymer (η_1 and η_2) depend on whether the condition (9), which depends on the applied voltage, is satisfied. Moreover, the ratio η_2/η_1 decreases with applied voltage. This is in complete agreement with experimental data.

The dependence of the wavelength of emitted light on the size of nanocrystals is not connected with the transport effects discussed above but, as is already generally accepted, is due to influence of size quantization on the energy levels in the nanocrystals.

A difference between photo- and electroluminescence spectra was observed only by some authors. For this reason its explanation presumably does not have a general character but is connected with some specific properties of a particular structure. For instance, one may assume that the size of nanocrystals, which determines the energy of emitted quanta, has a gradient in the growth direction. [1] In this case light emission from nanocrystals closer to the electrode with lower injection effectiveness will be stronger. At the same time, photopumping will excite all nanocrystals equally since the layer thickness is much less than the absorption length of the light. The alternative explanation of the red shift in electroluminescence in terms of reabsorption of radiation does not address the fact that the same reabsorption would exist in photoluminescence.

The formation of potential barriers around nanocrystals due to their recharging, described in Section 3, can account for long-term relaxation and memory effects. These phenomena are well known in inhomogeneous semiconductors [12,14,15] and are connected with charge separation by potential barriers.

The physical model discussed in the paper allows us to formulate some particular requirements which should be met in order to fabricate structures with the maximal effectiveness of luminescence in nanocrystals. Based on the results of Section 4 we make the following recommendations:

- The structures should have similar effectiveness of electron and hole injection ($\mu_n n_0 \approx \mu_p p_0$). Though for a given polymer it is presumably rather difficult to vary μ_n and μ_p independently, it may be possible to achieve this condition by a suitable choice of contact materials and technology which will determine n_0 and p_0.
- It is desirable to have high carrier mobilities, thin polymer films, and high applied voltages to satisfy the equality Eq. (9).
- If both the above-mentioned requirements cannot be satisfied, the layer containing nanocrystals must be placed as close as possible to the electrode with weaker injection (This condition was presumably satisfied in the asymmetric structures reported in Refs. [5,8]).

7. Conclusions

We have obtained a number of results of general utility in the area of composite organic–inorganic

[1] Contrary to our simple model, the layer containing nanocrystals in Ref. [5] had a considerable thickness of 25 nm which is 10 times greater than the nanocrystal diameter.

structures for electroluminescence. Our findings are useful in guiding and interpreting experiment and in designing devices with maximum luminescence efficiency.

It is worth revisiting some of the assumptions and simplifications introduced herein with a view to identifying avenues for further progress.

In this work, we have not dealt explicitly with the implications of field-dependent mobilities in conducting polymers, although our original specification of the problem does not preclude treatment of this issue. This effect may have important implications on device performance in light of the resulting self-consistent interplay between the field surrounding the nanocrystal and the local mobility in the polymer adjacent to the nanocrystal.

We have argued in this work that transport to the nanocrystals is the rate-limiting process in the system considered, in contrast with the situation in all-inorganic quantum dot structures in which capture into the quantum-confined states is the limiting process investigated intensively by a series of authors (see, e.g., Refs. [16–18]). Our assumption merits further careful consideration since the capture processes from a low-mobility organic bulk material into the inorganic nanocrystals may have their own peculiarities, and in some cases could play an essential role. A strong difference in vibrational spectra between polymers and inorganic crystals may change the properties of confined optical phonons. Such mechanisms would influence the severity of the phonon bottleneck and thereby play a role in carrier capture [19].

References

[1] Friend RH et al. Nature 1999;397:121.
[2] Hebner TR et al. Appl Phys Lett 1999;72:519.
[3] Colvin VL, Schlamp MC, Alivisatos AP. Nature 1994; 370:354.
[4] Greenham NC, Peng X, Alivisatos AP. Phys Rev B 1996;54:17628.
[5] Schlamp MC, Peng X, Alivisatos AP. J Appl Phys 1997;82:5837.
[6] Dabbousi BO, Rodriguez-Viejo J, Mikulec FV, Heine JR, Mattoussi H, Ober R, et al. J Phys Chem B 1997;101:9463.
[7] Dabbousi BO, Bawendi MG, Onitsuka O, Rubner MF. Appl Phys Lett 1995;66:1316.
[8] Mattoussi H, Radzilowski LH, Dabbousi BO, Thomas EL, Bawendi MG, Rubner MF. J Appl Phys 1998;83:7965.
[9] Asryan LV, Suris RA. Semicond Sci Technol 1996;11:554.
[10] Lampert MA, Mark P. Current injection in solids. New York: Academic Press; 1970.
[11] Shik AY. Sov Phys Semicond 1982;16:200.
[12] Shik A. Electronic properties of inhomogeneous semiconductors. New York: Gordon & Breach; 1995.
[13] Milnes AG. Deep impurities in semiconductors. New York: Wiley; 1973.
[14] Asryan LV, Suris RA. IEEE J Select Topics Quant Electron 1997;3:148.
[15] Shik AYa, Shmartsev YuV. In: Alferov ZI, editor. Semiconductor heterostructures: physical processes and application. Moscow: Mir; 1989.
[16] Ferreira R, Bastard G. Appl Phys Lett 1999;74:2818.
[17] Toda Y, Moriwaki O, Nishioka M, Arakawa Y. Phys Rev Lett 1999;82:4114.
[18] Marcinkevicius S, Lean R. Phys Scr 1999;T79:79.
[19] Xin Q-L, Nakayama H, Arakawa Y. Phys Rev B 1999;59:5069.